

# Current-voltage characteristics of Ag/TiO<sub>2</sub>/n-InP/Au Schottky barrier diodes

Cite as: J. Appl. Phys. **125**, 035704 (2019); doi: [10.1063/1.5064637](https://doi.org/10.1063/1.5064637)

Submitted: 6 October 2018 · Accepted: 1 January 2019 ·

Published Online: 18 January 2019



Ahmet Kürşat Bilgili,<sup>1</sup> Tamer Güzel,<sup>2</sup> and Metin Özer<sup>1</sup> 

## AFFILIATIONS

<sup>1</sup>Faculty of Science, Gazi University, 06500 Ankara, Turkey

<sup>2</sup>Mechatronics Department, Ömer Halisdemir University, Niğde, Turkey

## ABSTRACT

The effect of the TiO<sub>2</sub> interfacial layer on rectifying junction parameters of Ag/TiO<sub>2</sub>/n-InP/Au Schottky diodes has been investigated using current-voltage (I-V) measurements in the temperature range of 120–420 K with steps of 20 K. The barrier height is found to be 0.19 eV and 0.68 eV from current-voltage characteristics at 120 K and 420 K, respectively. At 120 K and 420 K, the ideality factor is found to be 3.52 and 1.01 for the Ag/TiO<sub>2</sub>/n-InP/Au Schottky barrier diode, respectively. These results are gained by the thermionic emission theory at room temperature. Values of series resistances gained from the Cheung-Cheung method are compared with results gained from a modified Norde method. These experimental results indicate that series resistance decreases with an increase in temperature. The current-voltage (I-V) measurements showed that the diode with the TiO<sub>2</sub> interfacial layer gave a double Gaussian property in the examined temperature range. The Richardson constant is also calculated from a modified Richardson plot and is found to be very compatible with the theoretical value. Interface state density is also examined by using I-V characteristics.

Published under license by AIP Publishing. <https://doi.org/10.1063/1.5064637>

## I. INTRODUCTION

Metal-Semiconductor (MS) structures are an important research area in the electronics industry. Formation and characterization of these structures may result in producing some useful technological devices. The reason why Schottky contacts attract much attention in the scientific world is because it is still not possible to explain correctly how the Schottky barrier is formed. Therefore, to understand and make a correct description of the Schottky barrier height (BH), many researchers make different investigations by using different materials and methods around the world. During these studies, different kinds of electronic devices are produced by researchers, such as optoelectronic devices, microwave devices, solar cells, detectors, and circuits with chips that can be used in qualified communication. In the electronics industry, MS contacts have a large application field. Results gained by measurements and calculations by using current-voltage (I-V) characteristics of MS structures are usually different from an ideal thermionic emission (TE) model. Therefore, examination of I-V characteristics only at room temperature is not enough for having knowledge about the barrier at the MS interface or conduction mechanisms of the diode. We can understand different

sides of conduction mechanisms by using temperature dependent I-V characteristics.<sup>1–3</sup> According to analysis results of I-V characteristics of surface behavior diagrams (SBDs), it is seen that there is a decrease in BH,  $\Phi_b$ , and an increase in the ideality factor  $n$  when the temperature decreases.<sup>4</sup>

The reason for the decrease in BH and the increase in the ideality factor when the temperature decreases is that other electrical abnormalities may be related to Schottky barrier height (SBH) inhomogeneity. Abnormal conduct in SBDs can be partly described by accepting that there are small regions with lower BH than the junction's main BH. This circumstance may affect the current across the MS contact with a great percentage. Tung and co-workers found larger ideality factors and smaller BHs when they increased the inhomogeneity of barriers.<sup>5–8</sup> Schottky barrier inhomogeneity, which means potential fluctuations at the top of the barrier, may be caused by field emission at the interface.<sup>9</sup> In many previous works, different operations are made in order to increase the naturally low BH of InP. Hattori and Izumi<sup>10</sup> deposited the P<sub>x</sub>O<sub>y</sub> compound as an interfacial layer. Wada et al.<sup>11</sup> showed that forming a very thin oxide layer between metal and InP caused a decrease in leakage current and an increase in BH.

Hasegawa<sup>12</sup> showed that the SBH can be increased by using interfacial layers and attempted to describe the mechanisms related to the increasing of BH by using Fermi level pinning. Davis and co-workers<sup>13</sup> investigated the effect of illumination over the interfacial layer and the changing in BH. Kamimura *et al.*<sup>14</sup> formed an oxide layer at the interface by etching the sample into the Bromur solution at room temperature. As a result of these studies, it is seen that electrical behaviors of the devices are strongly dependent on the preparation process of semiconductor surface for contact and choosing the most suitable metal. In the present study, Ag/TiO<sub>2</sub>/n-InP/Au Schottky barrier diodes were fabricated using the sputtering method with 120 Å thickness of the TiO<sub>2</sub> interfacial layer, after forming Au back contact on the n-InP substrate (Fig. 1). The purpose of adding TiO<sub>2</sub> on the interface is to examine its effect on device performance. Bilgili did this examination in his master's thesis for the first time in 2015<sup>15</sup> and found out that as the thickness of the TiO<sub>2</sub> layer decreases, diode parameters get more ideal. As TiO<sub>2</sub> is grown on the interface by the sputtering method, it diffuses over n-InP better and changes the work function. This results in improvement of device performance. The influence of the TiO<sub>2</sub> interlayer on p-InP is also not investigated by anyone in the literature. But the influence of it is investigated for p-Si. If an estimation is made, because of the negative charge of oxygen in TiO<sub>2</sub>, it will make a perfect contact on p-InP. It will affect the width of the depletion region, so the interface states and device performance will improve. I-V characteristics were measured and analyzed in the temperature range of 120–420 K by steps of 20 K.

## II. EXPERIMENTAL PROCEDURE

Schottky barrier diodes were prepared on a 500 μm thick n-type InP semiconductor with orientation (100) and carriers concentration of  $3.13 \times 10^{18} \text{ cm}^{-3}$ . The wafer was degreased consecutively in trichloroethylene, acetone, and methanol by using ultrasonic agitation for 5 min in each step. The degreased was etched with HF:H<sub>2</sub>O (1:10) for 30 s to remove native oxides on the surface. Back side ohmic contact was made by sputtering Au under  $1 \times 10^{-6}$  Torr pressure with a thickness of 150 nm. Then, samples were annealed at 325 °C for 4 min under a pure N<sub>2</sub> atmosphere. Before Schottky contacts of Ag, TiO<sub>2</sub> were deposited on the polished side of n-InP with a thickness of 120 Å. Schottky contacts with 0.75 mm

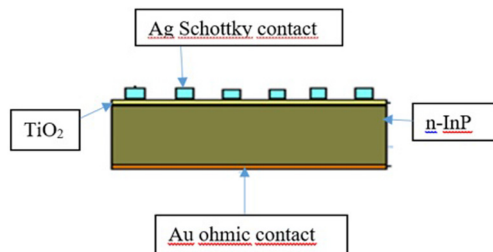


FIG. 1. The structure of the Ag/TiO<sub>2</sub>/n-InP/Au Schottky barrier diode.

diameter were formed on the TiO<sub>2</sub> film on the sample by using a shadow steel mask. I-V measurements of the devices were carried out using a Keithley 2400 sourcemeter in the temperature range of 120–420 K using a temperature controlled vpf-475 cryostat. Sample temperature was monitored using a thermocouple close to the sample, and the temperature is controlled with a Lake Shore model 321 autotuning temperature controller. Temperature stability for each run was better than 0.1 K.

## III. RESULTS AND DISCUSSION

### A. Current-voltage characteristics (I-V)

According to TE, the equation related to the current between metal and semiconductor is

$$I = I_0 \exp\left(\frac{q(V - IR)}{nKT}\right) \left[1 - \exp\left(-\frac{q(v - IR)}{kT}\right)\right]. \quad (1)$$

Here  $I_0$  is the saturation current.  $I_0$  is found by y axis intercept of the  $\ln(I)$ -V plot's linear part in the forward-bias region ( $V = 0$ ). Saturation current  $I_0$  is calculated by

$$I_0 = A A^{**} \exp\left(\frac{-q\Phi_{b0}}{kT}\right). \quad (2)$$

Here  $A$  is the diode area,  $\Phi_{b0}$  is the barrier height,  $A^*$  is the Richardson constant,  $k$  is the Boltzman constant, and  $T$  is the temperature. (For n-InP, the Richardson constant is  $9.4 \text{ A cm}^{-2} \text{ K}^{-2}$ .) By using Eq. (2),  $\Phi_{b0}$  can be calculated as

$$\phi_{b0} = \frac{kT}{q} \ln\left(\frac{AA^*T^2}{I_0}\right). \quad (3)$$

In the forward-bias region,  $\ln(I)$  vs.  $V$  plot is expected to be linear. If this plot is not linear, this means that the ideality factor is large and the diode is not an ideal diode. The reason for this may be the existence of an interfacial layer or recombination at the interface. The ideality factor can be calculated as<sup>16</sup>

$$n = \frac{q}{kT} \left(\frac{dV}{d\ln I}\right). \quad (4)$$

Current-voltage characteristics of the produced diode are shown in Fig. 2 in the temperature range of 120–420 K.

According to the TE model, the ideality factor is calculated by the slope of experimental  $\ln(I)$  vs.  $V$  plot. The barrier height at zero-bias is determined by the intercept of this plot. At 120 K and 420 K, the ideality factor is found to be 3.52 and 1.01 for the Ag/TiO<sub>2</sub>/n-InP/Au Schottky barrier diode, respectively. The barrier height is found to be 0.19 eV and 0.68 eV for the same diode at the same temperatures. The change of the ideality factor and the barrier height vs. temperature is shown in Fig. 3.

According to this plot, the ideality factor decreases and the barrier height increases with an increase in temperature.

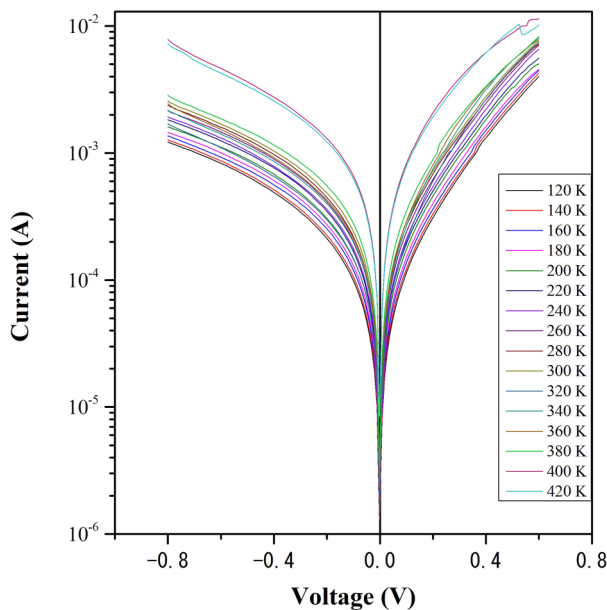


**FIG. 2.** Reverse and forward bias I-V characteristics of the Ag/TiO<sub>2</sub>/n-InP/Au Schottky diode as a function of temperature.

This result indicates that both parameters are strongly dependent on temperature. Because current transport across the MS interface is dependent on temperature, at low temperatures, the current is formed by the carriers which surmount the lower barriers. As a result, the dominant barrier height decreases and the ideality factor increases. At high temperatures, the opposite of this process comes out.

In general, the semilogarithmic I-V plot's forward-bias low voltage region shows linearity. However, when the voltage

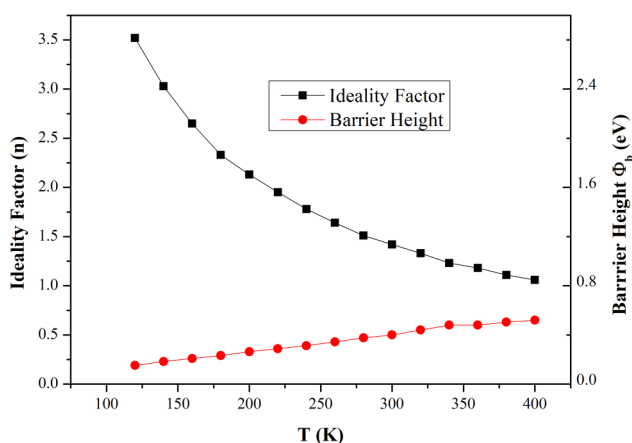


**FIG. 3.** Temperature dependence of the ideality factor and barrier height for the Ag/TiO<sub>2</sub>/n-InP/Au Schottky diode.

increases, a deviation from linearity occurs. Some of the reasons for this are interface states and resistance caused by the oxide layer. Series resistance is one of the important parameters to let us understand the electrical characteristics. In order to determine series resistance, there are different methods. The first of these methods is the Cheung-Cheung method. By using this method, it is possible to determine parameters, such as  $n$ ,  $R_s$ , and  $\Phi_b$ . These parameters are determined by  $dV/d(\ln I)$  vs.  $I$  and  $H(I)$ - $I$  function plots:<sup>17-19</sup>

$$dV/d(\ln I) = nkT/q + IR_s, \quad (5)$$

$$H(I) = IR_s + n\Phi_b. \quad (6)$$

As can be seen in Eqs. (5) and (6), the slope of  $dV/d(\ln I)$  vs.  $I$  plot (Fig. 4) gives us series resistance ( $R_s$ ) and intercept of  $y$  axis gives us the ideality factor ( $n$ ). Also, the slope of  $H(I)$  vs.  $I$  plot (Fig. 5) gives us series resistance and together with the ideality factor  $n$ , gained from  $dV/d(\ln I)$  vs.  $I$  plot, intercept point gives us ( $n\Phi_b$ ). We deduce  $\Phi_b$  from this intercept point. By using this method,  $n$ ,  $R_s$ , and  $\Phi_b$  are calculated. Results can be seen in Tables I and II.

Because of the large value of series resistance, in spite of  $\ln(I)$  vs.  $V$  plot, the Norde method is a more suitable method for determining the barrier height. This method is also improved for calculating series resistance. The only disadvantage of this method is the difficulty of determining the minimum point on the plot. According to the Norde method, the Norde function is given by the following equation,

$$F(V) = \frac{V}{\gamma} - \frac{1}{\beta} \ln \left( \frac{I(V)}{AA^{**}T^2} \right). \quad (7)$$

Here,  $\beta = q/kT$  and  $\gamma$  is an integer greater than ideality factor.

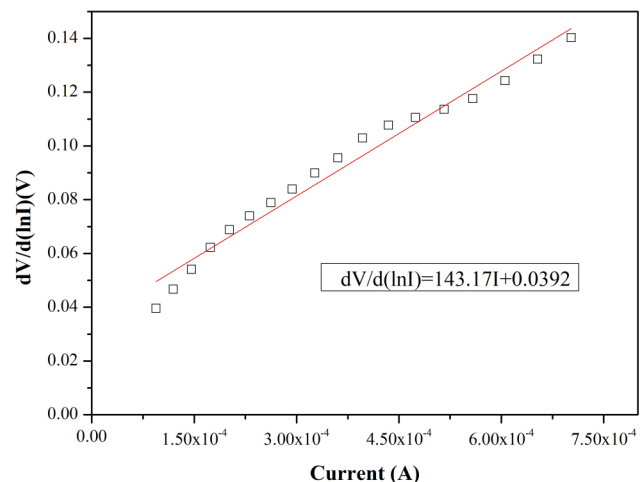


**FIG. 4.** Plot of  $dV/d(\ln I)$  versus  $I$  for the Ag/TiO<sub>2</sub>/n-InP/Au Schottky diode at room temperature.

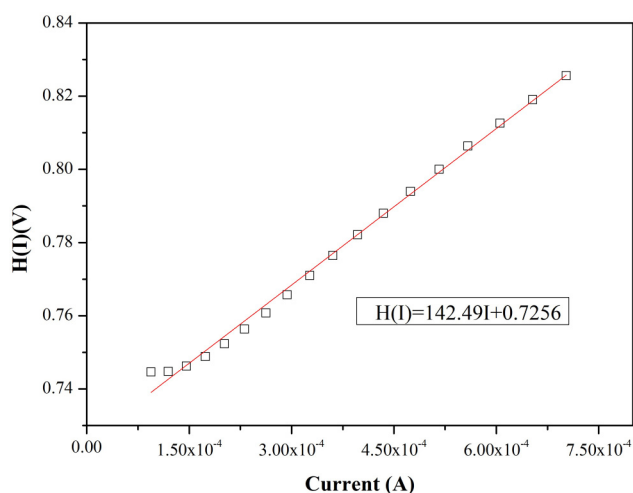


**FIG. 5.** Plot of  $H(I)$  versus  $I$  for the Ag/TiO<sub>2</sub>/n-InP/Au Schottky diode at room temperature.

$F(V)$  vs.  $V$  function has a minimum point as can be seen in Fig. 6,  $V_{\min}$  corresponds to  $F_{\min}$ . By using the following equation, the barrier height can be calculated

$$\varphi_b = F_{\min} + \frac{V_{\min}}{\gamma} - \frac{kT}{q}. \quad (8)$$

$I_{\min}$  corresponds to  $V_{\min}$  and  $R_s$  is calculated by the following equation,<sup>20,21</sup>

$$R_s = \frac{kT(\gamma - n)}{qI_{\min}}. \quad (9)$$

Results gained from this method are shown in Table III. As can be seen in Tables I–III, results gained from the Cheung-Cheung method and Norde method are in good agreement with each other.

Change of series resistance vs. temperature can be seen in Fig. 7. As can be seen in Fig. 7, series resistance decreases

**TABLE I.** Series resistance ( $R_s$ ) and ideality factor ( $n$ ) values according to the Cheung-Cheung method [ $dV/d(\ln I)$ ].

$T$ (K)	$R_s$ ( $\Omega$ )	$n$
120	307	3.87
140	282	3.42
160	273	2.86
180	239	2.62
200	213	2.33
220	194	2.16
240	186	1.9
260	158	1.81
280	146	1.65
300	143	1.51

**TABLE II.** Series resistance ( $R_s$ ) and barrier height ( $\Phi_b$ ) values according to the Cheung-Cheung method,  $H(I)-I$ .

$T$ (K)	$R_s$ ( $\Omega$ )	$\Phi_b$ (eV)
120	305	0.18
140	280	0.21
160	270	0.25
180	237	0.28
200	212	0.31
220	194	0.34
240	184	0.38
260	157	0.41
280	146	0.45
300	142	0.48

with an increase in temperature. This may be attributed to the higher energy of the carriers at higher temperatures so that they can move more freely toward the metal in the expanded interfacial layer with higher mobility.

An alternative method to calculate the barrier height is the Richardson plot (Fig. 8). The equation to draw this plot is

$$\ln\left(\frac{I_0}{T^2}\right) = \ln(AA^{**}) - \frac{q\Phi_{b0}}{kT}. \quad (10)$$

According to this equation,  $\ln(I_0/T^2)$  vs.  $1000/T$  plot is expected to give a straight line. The slope of this plot gives us the barrier height at  $T = 0$  K. This value is also called activation energy. The slope line intercept point of this plot gives us the Richardson constant ( $A^*$ ). For the Ag/TiO<sub>2</sub>/n-InP/Au Schottky barrier diode, the Richardson constant and activation energy are calculated as  $6.31 \times 10^{-7} \text{ A cm}^{-2} \text{ K}^{-2}$  and 0.23 eV, respectively.

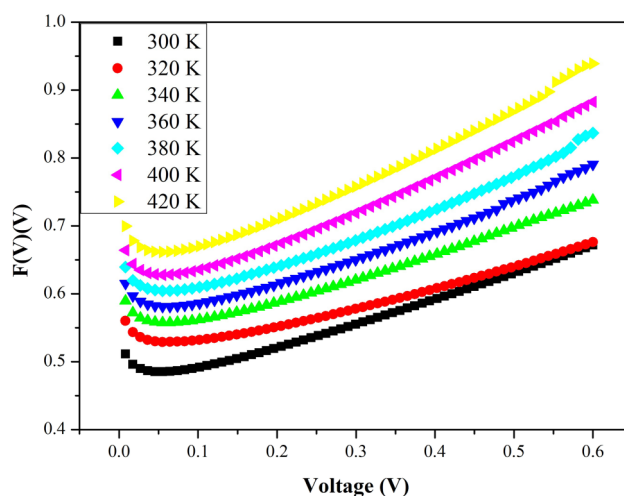


**FIG. 6.** Plot of  $F(V)$  versus  $V$  for the Ag/TiO<sub>2</sub>/n-InP/Au Schottky diode at 300–420 K.

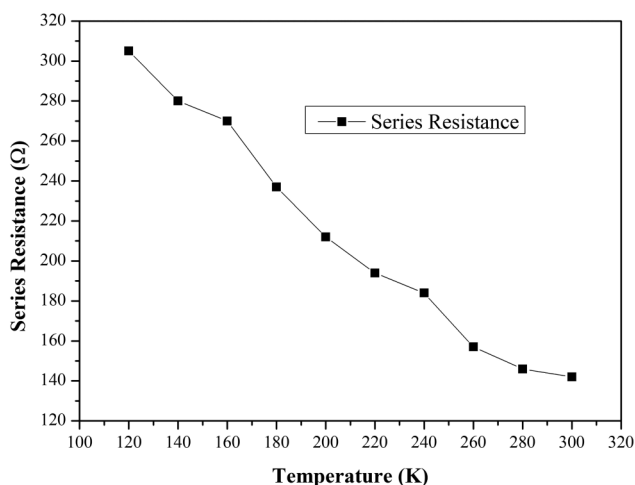
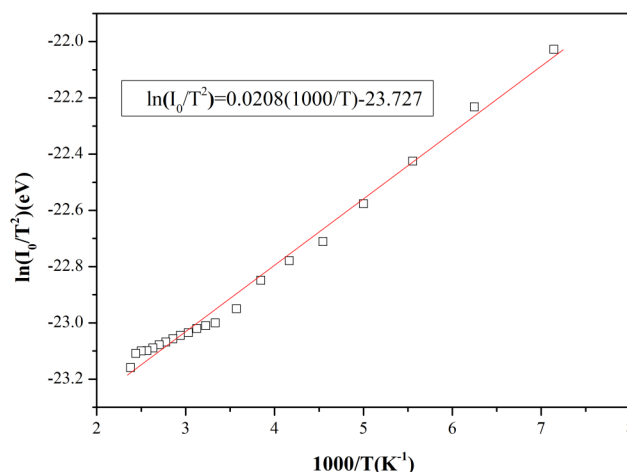
**TABLE III.** Series resistance ( $R_s$ ) and barrier height ( $\Phi_b$ ) values according to the Norde method.

Temperature (K)	$R_s$ ( $\Omega$ )	$\Phi_b$ (eV)
300	82	0.48
310	139	0.5
320	145	0.52
330	99	0.54
340	97	0.55
350	92	0.57
360	67	0.57
370	74	0.59
380	43	0.6
390	31	0.6
400	28	0.62
410	31	0.64
420	28	0.66

This result is found too different from the theoretical value of the Richardson constant. Deviation in the result gained from the Richardson plot may be attributed to barrier inhomogeneity. Devi and co-workers,<sup>22</sup> the Richardson constant  $A^*$  gained from I-V characteristics may be different from theoretical value because of the deviation in the calculated effective mass.

Plots for barrier height vs. ideality factor include two different linear parts. This may be explained by inhomogeneity in barrier heights.

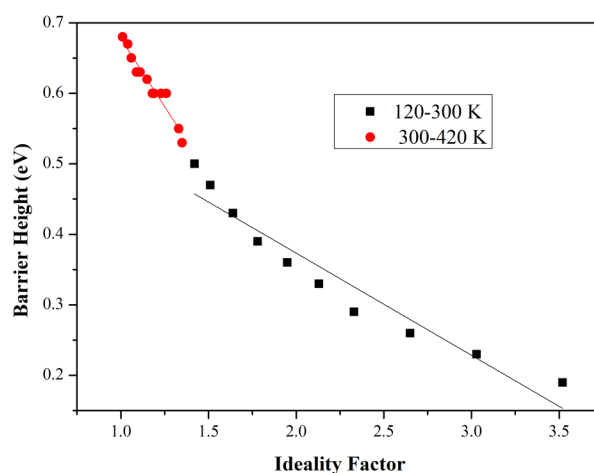
According to Fig. 9, homogeneous barrier heights are calculated by the intercept point on the barrier height axis for  $n=1$ . For the Ag/TiO<sub>2</sub>/n-InP/Au Schottky barrier diode, the barrier height is determined as 0.66 eV and 1.06 eV for 120–300 K and 300–420 K temperature ranges, respectively. These results indicate that the current transport mechanism has a deviation from the TE model.

**FIG. 7.** Temperature dependence of series resistance of the Ag/TiO<sub>2</sub>/n-InP/Au Schottky diode in the temperature range of 120–300 K.**FIG. 8.** Richardson plot of  $\ln(I_0/T^2)$  versus  $1000/T$  for the Ag/TiO<sub>2</sub>/n-InP/Au Schottky diode.

The Gaussian distribution model is introduced by Song and coworkers in order to explain these deviations from the TE model. Vanalme *et al.* investigated double Gaussian in InP Schottky barriers in detail and this study is made in accordance with that study.<sup>23</sup> According to them, in the base of the deviations from the TE model, there is the spatial homogeneity of barrier heights. Spatial inhomogeneity is given by

$$P(\Phi_{b0}) = \frac{1}{\sigma_0 \sqrt{2\pi}} \exp \left[ -\frac{(\Phi_{b0} - \bar{\Phi}_{b0})^2}{2\sigma_0^2} \right]. \quad (11)$$

Here,  $P(\Phi_{b0})$  is the Gaussian distribution,  $(\bar{\Phi}_{b0})$  is the mean barrier height, and  $(\sigma_0)$  is the standard deviation.<sup>24,25</sup> According

**FIG. 9.** The zero-bias barrier height versus the ideality factor for the Ag/TiO<sub>2</sub>/n-InP/Au Schottky barrier diode in the temperature range of 120–420 K.



to this equation, the current through the diode is given by

$$I(V) = \int_{-\infty}^{\infty} I(\Phi_{b0}, V) P(\Phi_{b0}) d\Phi. \quad (12)$$

If the term  $I(\Phi_{b0}, V)$  in this equation is modified,

$$I(V) = AA * \exp\left[-\frac{q}{kT} \left(\bar{\Phi}_{b0} - \frac{q\sigma_0^2}{2kT}\right)\right] \exp\left(\frac{qV}{n_{ap}kT}\right) \times \left[1 - \exp\left(\frac{qV}{kT}\right)\right], \quad (13)$$

the equation is found. Here, the saturation current  $I_0$  is calculated by the following equation:

$$I_0 = AA * \exp\left(-\frac{\Phi_{ap}}{kT}\right). \quad (14)$$

According to this model,

$$\Phi_{ap} = \bar{\Phi}_{b0}(T=0) - \frac{q\sigma_0^2}{2kT}. \quad (15)$$

Because temperature dependence of  $\sigma_0$  is small it may be neglected. Temperature dependence of ideality factor is given by

$$\left(\frac{1}{n_{ap}} - 1\right) = -\rho_2 + \frac{q\rho_3}{2kT}. \quad (16)$$

Here,  $n_{ap}$  is the experimental value of ideality factor.  $\rho_2$  and  $\rho_3$  are voltage deformations of the BH. There is a linear relation among  $\rho_2$ ,  $\rho_3$ , and  $\sigma_0$ . So following equations can be written as

$$\bar{\Phi}_b = \bar{\Phi}_{b0} + \rho_2 V, \quad (17)$$

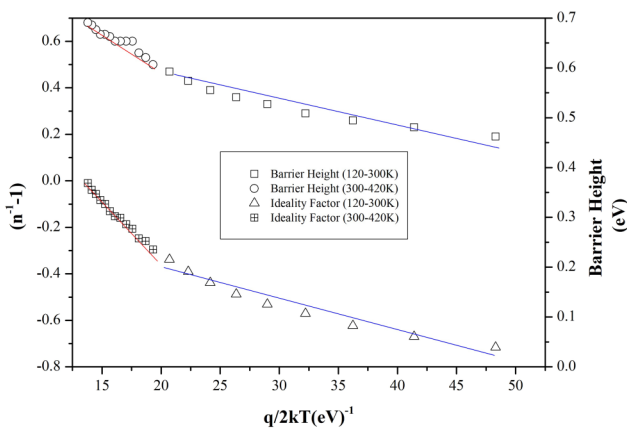


**FIG. 10.** The zero-bias barrier height and ideality factor versus  $q/2kT$  curves and their linear fits for the Ag/TiO<sub>2</sub>/n-InP/Au Schottky contact according to the Gaussian distribution of the barrier heights.

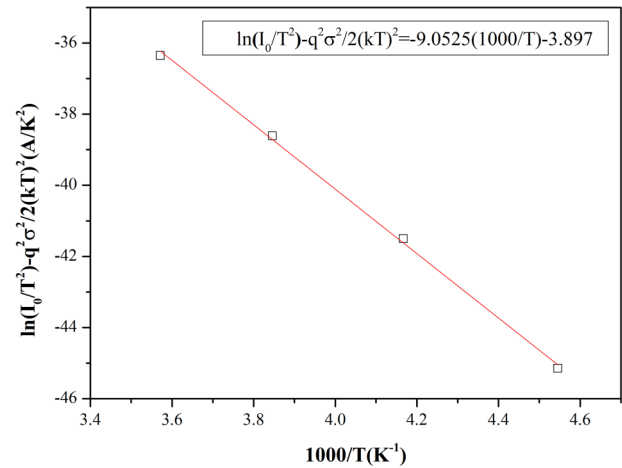


**FIG. 11.** Modified Richardson  $\ln(I_0/T^2) - q^2\sigma_0^2/2k^2T^2$  versus  $1000/T$  plot for the Ag/TiO<sub>2</sub>/n-InP Schottky diode according to the Gaussian distribution of the barrier heights at low temperatures.

$$\sigma_{0s} = \sigma_{0c} + \rho_3 V. \quad (18)$$

If  $\sigma_0$  is small, the barrier height is more homogeneous. According to Eqs. (14) and (15),  $\Phi_{ap}$  vs.  $q/2kT$  plot is expected to give a straight line. The slope of this line gives us  $\sigma_0$ , and the intercept point on the y axis gives us the mean barrier height ( $\bar{\Phi}_{b0}$ ). Also,  $(n_{ap}^{-1}-1)$  vs.  $q/2kT$  plot is expected to be a straight line.<sup>26-28</sup> The slope of this line is  $\rho_3$ , and the intercept point on the y axis is  $\rho_2$ .  $\Phi_{ap}$  vs.  $q/2kT$  and  $(n_{ap}^{-1}-1)$  vs.  $q/2kT$  plots can be seen in Fig. 10.

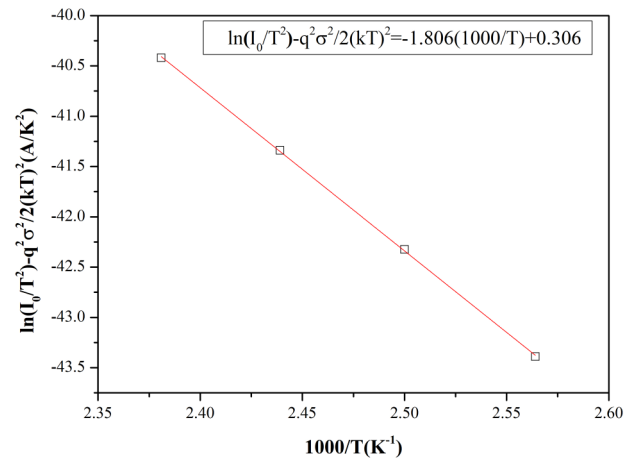


**FIG. 12.** Modified Richardson  $\ln(I_0/T^2) - q^2\sigma_0^2/2k^2T^2$  versus  $1000/T$  plot for the Ag/TiO<sub>2</sub>/n-InP Schottky diode according to the Gaussian distribution of the barrier heights at high temperatures.

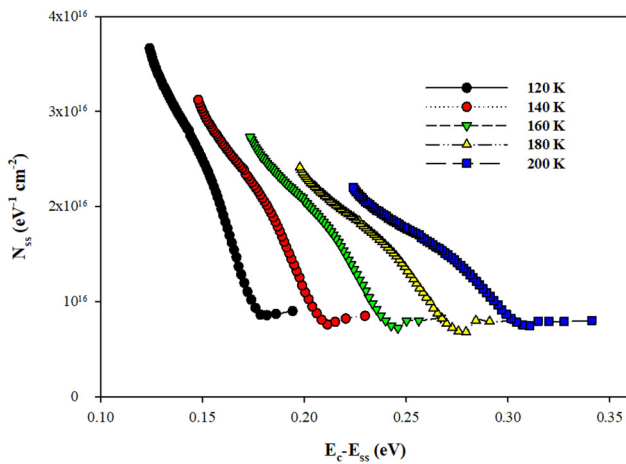


**FIG. 13.** Interface state density distribution profile as a function of  $E_c - E_{ss}$  for the Ag/TiO<sub>2</sub>/n-InP Schottky diode at 120–200 K temperature range.

( $\Phi_{b01}$ ),  $\sigma_{01}$ ,  $\rho_2$ , and  $\rho_3$  are determined as 0.69 eV, 138 mV,  $-0.1125$  V, and  $-0.0134$  V in 120–300 K temperature range, respectively. ( $\Phi_{b02}$ ),  $\sigma_{02}$ ,  $\rho_2$ , and  $\rho_3$  are determined as 1.25 eV, 257 mV, 0.6634 V, and  $-0.0498$  V in 300–420 K temperature range, respectively. For the Ag/TiO<sub>2</sub>/n-InP/Au Schottky barrier diode, the calculated mean barrier heights and standard deviations are too large to neglect, especially in the low temperature range. This situation implies that barrier distribution is inhomogeneous. If the Richardson equation is modified, the following equation is deduced:

$$\ln\left(\frac{I_0}{T^2}\right) - \left(\frac{q^2\sigma^2}{2k^2T^2}\right) = \ln(AA^*) - \frac{q\Phi_{b0}}{kT}. \quad (19)$$

$\ln(I_0/T^2) - q^2\sigma_0^2/2k^2T^2$  vs.  $1000/T$  plot is expected to be

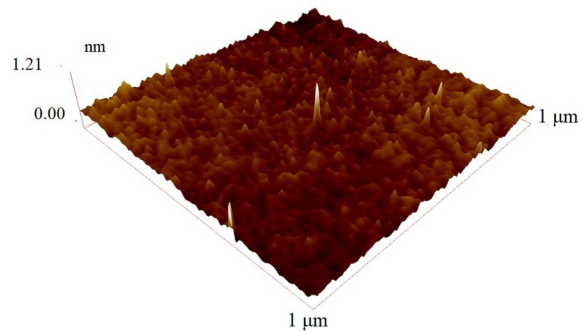
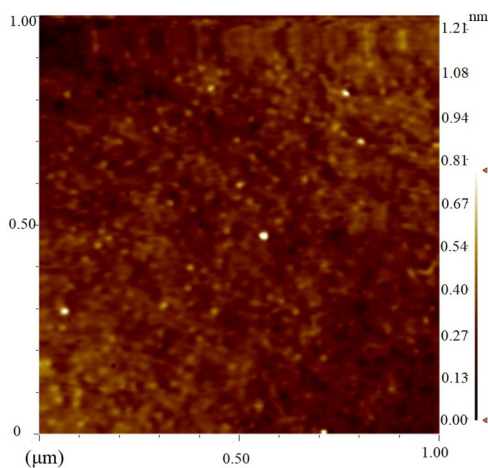


**FIG. 14.** AFM micrographs of the Ag/TiO<sub>2</sub>/n-InP Schottky contacts as-deposited.

linear, the slope of this plot gives  $\Phi_b$  and intercept point on the y axis is the Richardson constant  $A^*$  (Figs. 11 and 12).<sup>29–31</sup>

For the Ag/TiO<sub>2</sub>/n-InP/Au Schottky barrier diode,  $\Phi_b$  and  $A^*$  are determined as 0.78 eV and  $2.58 \text{ A cm}^{-2} \text{ K}^{-2}$  in 120–300 K temperature range and 1.39 eV and  $20 \text{ A cm}^{-2} \text{ K}^{-2}$  in 300–420 K temperature range, respectively. These results for the Richardson constant are in good agreement with theoretical value.

Other effects influencing the current transport mechanism together with semiconductor's electrical properties are the thickness of the interfacial layer and interfacial state density. Especially in determining the barrier height and the ideality factor, the interface state density ( $N_{ss}$ ) plays a significant role. If the interfacial layer is thick enough, the probability of conduction between metal and semiconductor is small. For this reason, the effective barrier height  $\Phi_e$  is dependent on the applied voltage.  $\Phi_e$  is calculated by the following equation:

$$\Phi_e = \Phi_{b0} + \left(\frac{d\Phi_e}{dV}\right)V = \Phi_{b0} + \beta V. \quad (20)$$

Here,  $\beta = 1 - [1/n(V)]$  and it implies the change of effective barrier height with voltage. Also, the change of the ideality factor with voltage is described by Card and Rhoderick. According to them,  $n(V)$  is calculated by the following equation:

$$n(V) = 1 + \frac{\delta}{\epsilon_i} \left[ \frac{\epsilon_s}{W_D} + qN_{ss} \right]. \quad (21)$$

Here,  $W_D$  is the depletion region width,  $\delta$  is the interfacial layer thickness,  $\epsilon_s$  and  $\epsilon_i$  are the dielectric constants of the semiconductor and interfacial layer, respectively.  $N_{ss}$  is the interface state density. By using Eq. (22),  $N_{ss}$  can be

calculated as follows:

$$N_{ss}(V) = \frac{1}{q} \left[ \frac{\epsilon_i}{\delta} (n(V) - 1) - \frac{\epsilon_s}{W_D} \right]. \quad (22)$$

The difference between the bottom edge of the conduction band and interfacial state density energy is calculated as follows:<sup>27</sup>

$$E_c - E_{ss} = q(\Phi_e - V). \quad (23)$$

The plot  $N_{ss}$  vs.  $E_c - E_{ss}$  can be seen in Fig. 13 in the 120–200 K temperature range. This plot may be deduced from the forward bias of I–V characteristics. As can be seen in Fig. 13, the values of  $N_{ss}$  are approximately between  $25 \times 10^{15}$  and  $9 \times 10^{15} \text{ cm}^{-2} \text{ eV}^{-1}$  at 200 K and between  $38 \times 10^{15}$  and  $8 \times 10^{15} \text{ cm}^{-2} \text{ eV}^{-1}$  at 120 K. This means that the interface state density decreases with an increase in temperature as expected.

Atomic force microscopy (AFM) was employed to characterize the surface morphology of the n-InP wafer. The AFM image of the chemically cleaned n-InP wafer is shown in Fig. 14. Surface morphology of the cleaned sample is fairly smooth with a root mean square (RMS) roughness of 0.0668 nm as shown in Fig. 14.

#### IV. CONCLUSION

In summary, electrical properties of Ag/TiO<sub>2</sub>/n-InP/Au Schottky diodes have been investigated by I–V measurements as a function of temperature. The barrier height is found to be 0.19 eV and 0.68 eV from current-voltage characteristics at 120 K and 420 K, respectively. With a decrease in temperature down to 120 K, BH decreases to 0.190 eV. Moreover, a modified Norde's function is used to calculate diode parameters including BHs and series resistance. Modification of the interfacial potential barrier of Ag/TiO<sub>2</sub>/n-InP/Au is achieved by using a thin TiO<sub>2</sub> interlayer. A change in the barrier height and ideality factor upon increasing temperature of 120 K to 420 K may be ascribed to the pinholes that might be formed in the TiO<sub>2</sub> interlayer. These pinholes may be formed during the growth period of the structure. There may occur dislocation lines because of lattice mismatch or the difference in thermal expansion coefficients. At the end point of these lines on the interface, there formed a hole like tiny dots called pinholes. Pinholes act as a tip of a pipe and help increase the mobility of charges. The obtained results show that the interface state density and series resistance have a significant effect on the electrical characteristics of the produced diode. The Richardson coefficient and the mean barrier height are also calculated by using the modified Richardson plot, and they are found in good agreement with the literature.

#### REFERENCES

- <sup>1</sup>H. Çetin and E. Ayyıldız, "Temperature dependence of electrical parameters of the Au/n-InP Schottky barrier diodes," *Semicond. Sci. Technol.* **20**, 625–631 (2005).

- <sup>2</sup>M. Özer, D. E. Yıldız, Ş. Altındal, and M. M. Bülbül, "Temperature dependence of characteristic parameters of the Au/SnO<sub>2</sub>/n-Si (MIS) Schottky diodes," *Solid State Electron.* **51**(6), 941–949 (2007).
- <sup>3</sup>D. E. Yıldız, Ş. Altındal, Z. Tekeli, and M. Özer, "The effects of surface states and series resistance on the performance of Au/SnO<sub>2</sub>/n-Si and Al/SnO<sub>2</sub>/p-Si (MIS) Schottky barrier diodes," *Mater. Sci. Semicond. Process.* **13**(1), 34–40 (2010).
- <sup>4</sup>F. E. Cimilli, M. Sağlam, H. Efeoglu, and A. Türüt, "Temperature dependent current voltage characteristics of the Au/n-InP diodes with inhomogeneous Schottky barrier height," *Physica B* **404**, 1558–1562 (2009).
- <sup>5</sup>R. T. Tung, "Electron transport at metal-semiconductor interfaces: General theory," *Phys. Rev. B* **45**, 509–522 (1992).
- <sup>6</sup>V. R. Reddy, A. Umapathi, and L. Dasaradha Rao, "Effect of annealing on the electronic parameters of Au/poly(ethylmethacrylate)/n-InP Schottky diode with organic interlayer," *Curr. Appl. Phys.* **13**, 1604–1610 (2013).
- <sup>7</sup>V. R. Reddy, "Electrical properties of Au/Polyvinylidene fluoride/n-InP Schottky diode with polymer interlayer," *Thin Solid Films* **556**, 300–306 (2014).
- <sup>8</sup>H. Çetin, E. Ayyıldız, and A. Türüt, "Barrier height enhancement and stability of the Au/n-InP Schottky barrier diodes oxidized by absorbed water vapor," *J. Vac. Sci. Technol. B* **23**(6), 2436 (2005).
- <sup>9</sup>J. H. Werner and H. H. Güttler, "Barrier inhomogeneities at Schottky contacts," *J. Appl. Phys.* **69**, 1522 (1991).
- <sup>10</sup>K. Hattori and Y. Izumi, "The electrical characteristics of degenerate InP Schottky diodes with an interfacial layer" *J. Appl. Phys.* **53**, 6906 (1982).
- <sup>11</sup>O. Wada, A. Majerfield, and P. N. Robson, "InP Schottky contacts with increased barrier height," *Solid State Electron.* **25**, 381–387 (1982).
- <sup>12</sup>H. Hasegawa, "Fermi level pinning and Schottky barrier height control at metal-semiconductor interfaces of InP and related materials," *Jpn. J. Appl. Phys.* **38**(Pt. 1, No. 2B), 1098–1102 (1999).
- <sup>13</sup>R. F. Davis, G. Kelner, M. Shur, J. W. Palmour, and J. A. Edmond, "Thin film deposition and microelectronic and optoelectronic device fabrication and characterisation in monocrystalline alpha and beta silicon carbide," *Proc. IEEE* **79**, 5 (1996).
- <sup>14</sup>K. Kamimura, T. Suzuki, and A. Kunioka, "InP metal-insulated semiconductor Schottky contacts using surface oxide layers prepared with bromine water," *J. Appl. Phys.* **51**, 4905–4907 (1980).
- <sup>15</sup>A. K. Bilgili, "Investigating the electrical properties of metal semiconductor contacts prepared on n-InP semiconductor with TiO<sub>2</sub> interfacial layer," M.Sc. thesis (Gazi University, 2015), Thesis number: 395660.
- <sup>16</sup>H. Çetin and E. Ayyıldız, "Electrical characteristics of Au, Al, Cu/n-InP Schottky contacts formed on chemically cleaned and air exposed n-InP surface," *Physica B* **394**, 93–99 (2007).
- <sup>17</sup>W. C. Dautremont Smith, P. A. Barnes, and J. W. Stayt, "A nonalloyed, low specific resistance Ohmic contact to n-InP," *J. Vac. Sci. Technol. B* **2**, 620 (1984).
- <sup>18</sup>T. S. Huang and R. S. Fang, "Barrier height enhancement of Pt/n-InP Schottky diodes by P<sub>2</sub>S<sub>5</sub>/(NH<sub>4</sub>)<sub>2</sub>S solution treatment of the InP surface," *Solid State Electron.* **37**(8), 1461–1466 (1994).
- <sup>19</sup>A. Singh and P. Cova, "Reverse I–V and C–V characteristics of Schottky barrier type diodes on Zn doped InP epilayers grown by metalorganic vapor phase epitaxy," *J. Appl. Phys.* **76**(4), 2336–2342 (1994).
- <sup>20</sup>Y. S. Ocak, M. Kulakci, R. Turan, T. Kılıcoglu, and O. Gullu, "Analysis of electrical and photoelectrical properties of ZnO/p-InP heterojunction," *J. Alloys Compd.* **509**(23), 6631–6634 (2011).
- <sup>21</sup>S. S. Naik, R. V. Reddy, C. J. Choi, and J. S. Bae, "Electrical and structural properties of double metal structure Ni/V Schottky contacts on n-InP after rapid thermal process," *J. Mater. Sci.* **46**, 558–565 (2010).
- <sup>22</sup>L. V. Devi, I. Jyothi, and R. V. Reddy, "Analysis of temperature dependent Schottky barrier parameters of Cu-Au Schottky contacts to n-InP," *Can. J. Phys.* **90**, 73–81 (2011).
- <sup>23</sup>G. M. Vanalme, L. Goubert, R. L. Van Meirhaeghe, F. Cardon, and P. Van Daele, "A ballistic electron emission microscopy study of barrier height inhomogeneities introduced in Au/III–V semiconductor Schottky



barrier contacts by chemical pretreatments," *Semicond. Sci. Technol.* **14**, 871 (1999).

<sup>24</sup>B. Zatko, F. Dubecky, O. Prochazkova, and V. Necas, "Role of electrode metalization in the performance of bulk semi-insulating InP radiation detectors," *Nucl. Instrum. Methods Phys. Res.* **576**(1), 98–102 (2007).

<sup>25</sup>E. Hökelek and G. Y. Robinson, "Schottky contacts on chemically etched p- and n-type indium phosphide" *Appl. Phys. Lett.* **40**, 426 (1998).

<sup>26</sup>M. Yıldırım, A. Eroğlu, Ş. Altındal, and P. Durmuş, "On the profile of temperature and voltage dependence of interface states and resistivity in Au/n-Si structure with 79 Å insulator layer thickness," *J. Optoelectron. Adv. Mater.* **13**(1), 98–105 (2011).

<sup>27</sup>B. Akkal, Z. Benamara, A. Boudissa, N. B. Bouiadjra, M. Armani, L. Bideux, and B. Gruzza, "Modelization and characterization of Au/InSb/InP

Schottky systems as a function of temperature," *Mater. Sci. Eng. B* **55**(3), 162–168 (1998).

<sup>28</sup>M. Soyulu and B. Abay, "Barrier characteristics of gold Schottky contacts on moderately doped n-InP based on temperature dependent I-V and C-V measurements," *Microelectron. Eng.* **86**(1), 88–95 (2009).

<sup>29</sup>R. V. Reddy, P. S. M. Reddy, A. Kumar, and C. J. Choi, "Effect of annealing temperature on electrical properties of Au/polyvinyl alcohol/n-InP Schottky barrier structure," *Thin Solid Films* **520**(17), 5715–5721 (2012).

<sup>30</sup>R. Padma, K. Latha, R. V. Reddy, and C. J. Choi, "Rapid thermal annealing effects on the electrical and structural properties of Ru/V/n-InP Schottky barrier diode," *Superlattices Microstruct.* **83**, 48–60 (2015).

<sup>31</sup>T. Guzel, A. K. Bilgili, and M. Ozer, Investigation of inhomogeneous barrier height for Au/n-type 6H-SiC Schottky diodes in a wide temperature range, *Superlattices Microstruct.* **124**, 30–40 (2018).